40   **1. INTRODUCTION**

41   Variation in D/H ratios (δD values) of thermogenic natural gases is often attributed to kinetically-controlled

42   fractionation during pyrolysis of kerogen or oils. A number of studies have investigated how D/H ratios of

43   methane and other hydrocarbons evolve with increasing maturity (Sackett, 1978; Berner et al., 1995; Sackett and

44   Conkright, 1997; Tang et al., 2005; Ni et al., 2011; Reeves et al., 2012). However, kinetic isotope effects

45   involving hydrogen addition or abstraction are often large and by themselves do not explain the geologically-

46   reasonable apparent equilibrium temperatures of ~150 to 220 °C obtained for reservoir gases that have been

47   studied for their clumped isotopologue compositions (Stolper et al., 2014, 2015; Wang et al., 2015; Douglas et al.,

48   2017; Young et al., 2017; Shuai et al., 2018; Giunta et al., 2019; Labidi et al., 2020; Thiagarajan et al., 2020).

49   There is also evidence that δD values of CH_4 approach values expected for isotopic equilibrium between CH_4 and

50   H_2O in formation waters at temperatures characterizing reservoirs and/or mature source rocks (~150 to 250 °C)

51   (Clayton, 2003; Wang et al., 2015; Xie et al., 2021), although findings of insignificant hydrogen exchange

52   occurring under these conditions also exist (Yeh and Epstein, 1981). In order for methane samples to have

53   approached or attained equilibrium values of $\Delta^{13}CH_3D$ and $\Delta^{12}CH_2D_2$—parameters that describe the abundances

54   of clumped isotopologues relative to a stochastic population of molecules containing isotopes randomly

55   distributed amongst them—there must be a pathway by which either (*i*) isotopes can be exchanged amongst

56   methane isotopologues alone, (*ii*) methane isotopologues exchange hydrogen with water or other organic

57   molecules, or (*iii*) methane isotopologues are derived from methyl moieties which contain C–H bonds that have

58   previously exchanged with water prior to forming methane (Hoering, 1984; Smith et al., 1985; Schimmelmann et

59   al., 1999, 2006; Lis et al., 2006).

60   Here, we study the origin of C–H bonds in thermogenic methane by heating kerogen in the presence of D_2O and

61   examining the degree of deuteration in the generated methane. This experiment is conceptually very similar to

62   ones conducted by Hoering (1984), Lewan (1997), and Schimmelmann et al. (2001). The experiments in those

63   studies were designed to track incorporation of D into bitumen and kerogen. None of these studies specifically

64   quantified the extent of deuteration in the produced natural gases.

3

65   **2.   METHODS**

66   **2.1.   Experimental methods**

67   Experiments were conducted in a gold-titanium reaction cell housed within a flexible cell hydrothermal apparatus

68   (Seyfried et al., 1987) at WHOI. Prior to use, the titanium surfaces in contact with the reaction cell contents were

69   heated in air for 24 h at 400 °C to form a more inert TiO_2 surface layer. The reaction cell was further pre-treated

70   prior to loading by soaking in concentrated HCl for 4 hours, followed by rinsing with water to pH neutral and

71   drying in the oven. The exit tube of the apparatus was cleaned by forcing ~20 ml of MilliQ deionized water

72   (18.2 MΩ) through, followed by ~20 ml concentrated HCl, ~100 ml water, ~20 ml concentrated HNO_3, and then

73   ~100 ml of water until the pH tested 7 using pH paper.

74   The source material for this experiment was a hand sample of Upper Cretaceous Eagle Ford Shale taken from an

75   outcrop in Uvalde County, Texas, USA (Hentz and Ruppel, 2010). There is no known oil or gas production from

76   the Eagle Ford in Uvalde County (Tian et al., 2013; *IHS Markit Well Database*, 2019). The Eagle Ford here is

77   thermally-immature (R_o = 0.40–0.55%, Cardneaux, 2012; Cardneaux and Nunn, 2013; Harbor, 2011). The sample

78   was powdered to <250 μm and Soxhlet-extracted to remove bitumen and free hydrocarbons. In a subsequent step,

79   the solvent-extracted residue was subjected to hydrochloric acid treatment to remove carbonate minerals.

80   Elemental analysis (**Table 1**) of the original rock sample (UNEX), the Soxhlet-extracted rock sample (EX), and

81   the decalcified+extracted rock sample (DECA) indicates a total organic carbon (TOC) content of ~2.5% and a

82   carbonate content of ~80% by weight. The H/C atomic ratio of the decalcified rock is 2.4. This value is probably

83   several tens of percent higher than the actual H/C ratio of isolated kerogen (not determined) given that substantial

84   amounts of H are likely borne by clays and other minerals that were not removed (Whelan and Thompson-Rizer,

85   1993; Baskin, 1997).

86   Geochemical data for the Eagle Ford sample can be drawn from neighboring Kinney County, Texas, where

87   complete sections of immature Eagle Ford have been recovered by the U.S. Geological Survey (drill core GC-3;

88   French et al., 2020) and Shell (Iona-1 drill core; Eldrett et al., 2014, 2015; Sun et al., 2016); there, the Eagle Ford

113 Concentrations of total dissolved inorganic carbon (ΣCO_2) and C_1 to C_6 hydrocarbons (alkanes and alkenes) were

114 determined using a purge-and-trap cryofocusing device coupled to a gas chromatograph equipped with a Porapak

115 Q column and serially-connected thermal conductivity and flame ionization detectors. Analytical procedures were

116 as described in Reeves et al. (2012). Analytical reproducibility on duplicate samples was $\pm 5\%$ or better (2σ). The

117 C_5 and C_6 compounds could not be quantified accurately due to their semi-volatile nature; however, C_5 and C_6

118 were detected at all sampling points.

119 At each sampling, a separate ~1 to 2 ml aliquot was injected directly into a pre-weighed, evacuated serum vial

120 capped with boiled blue butyl rubber stoppers, for analysis of the extent of deuteration of methane. A Hewlett-

121 Packard (HP) 6890 gas chromatography-mass spectrometry (GC-MS) system equipped with a 5Å molecular sieve

122 column (HP-PLOT 30 m × 0.32 mm × 12.0 μm) coupled to an HP 5973 mass selective detector was used to

123 determine the amount of deuteration in CH_4. Mass spectrometer source and quadrupole analyzer temperatures

124 were 230 and 150 °C, respectively, and mass spectra were recorded with an electron impact (EI) ionization energy

125 of 70 eV. Ion currents were monitored at integral masses between m/z 10 and 50. Extracted ion currents were

126 quantified at m/z 14 through 20 for methane. Expected fragmentation patterns of the five methane-d_n

127 isotopologues (C^1H_4, CH_3D, CH_2D_2, CHD_3, and CD_4) were determined by analysis of commercial synthetic

128 standards (>98% purity, Cambridge Isotope Laboratories, Inc.). We refer to the fully protiated methane

129 isotopologue as C^1H_4 in the text when it is necessary to specifically distinguish it from bulk CH_4.

3. RESULTS AND DISCUSSION

3.1. Temperature and thermal maturity

132 Temperatures logged during the experiment are shown in **Fig. 1A**. Using the temperature history, we calculated

133 thermal maturity as a function of time in units of vitrinite reflectance (%R_o) using EASY%Ro (Sweeney and

134 Burnham, 1990). The estimated thermal maturities are plotted in **Fig. 1B**. While the model predicts maturities of

135 ~0.20 to 0.34% R_o-equivalent for time points #1 and 2 (respectively) and the data are plotted at these calculated

136 maturities, the actual maturity at these time points can be no less than 0.4–0.5% (the initial maturity of the Eagle

6

Page: 8

Author: Subject: Highlight   Date: 4/21/2022 3:26:26 AM

Recommend plotting the initial maturity as a horizontal line on the plot in Figure 1B.

137 Ford rock sample, see §2.1). The difference between the plotted and actual %R_o values is somewhat immaterial;

138 what is key is that time points #1 and 2 represent kerogen that has undergone only incipient organic

139 metamorphism. Maturities encountered in remainder of the experiment spanned the entire range of the oil

140 window (ca. 0.5% to 1.3% R_o-equivalent; Burnham, 2019). The equivalent maturity at the final time point (#9) is

141 1.27% R_o.

142 **3.2.   Concentrations of aqueous species**

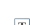143 *3.2.1.   Inorganic species*

144 Measured concentrations of aqueous species are shown in **Fig. 2**. Concentrations of aqueous H_2 increased from

145 below detection (<13 μmol/kg) to up to 1.1 mmol/kg at the end of the experiment, and increased with each

146 temperature step. The H_2 concentration also rose slightly between the beginning and end of each temperature

147 stage of the experiment.

148 The concentration of ΣCO_2 increased during the early stages of the experiment, and leveled off at ~50 mmol/kg at

149 350 °C. The plateauing inorganic carbon concentration suggests that the aqueous solution reached saturation with

150 carbonate minerals (Seewald et al., 1998), a result of CO_2 production during hydrothermal alteration of kerogen

151 (Seewald, 2003), and dissolution of carbonate minerals initially present in the Eagle Ford shale.

152 *3.2.2.   Alkanes and alkenes*

153 Concentrations of methane increased in every successive time step, as did concentrations of detected *n*-alkanes.

154 Except for the beginning of the experiment, molar concentrations of C_1 and ΣC_{2-4} were very similar and increased

155 almost in unison.

156 Alkenes (ethylene and propylene, **Fig. 2D–E**) rose in concentration with every increase in temperature, indicating

157 generation of unsaturated hydrocarbons via thermolytic processes. While concentrations of *n*-alkanes increased

158 monotonically from the beginning to end of each temperature stage, the concentrations of alkenes remained

159 constant—or in the 350 °C stage, trended downwards—with time during each stage. Concentrations of alkenes

7

160 consistent with thermodynamic equilibrium at measured H_2 concentrations are on the order of ~$10^{-7.4}$ and ~$10^{-6.6}$

161 mol/kg for ethylene and propylene, respectively, at 350 °C (Shock et al., 1989; Shock and Helgeson, 1990).

162 Measured concentrations of alkenes were ~2 orders of magnitude higher than alkane-alkene equilibrium

163 predictions, indicating strong disequilibrium in the relative concentration of alkenes and alkanes.

164 Evidence from hydrothermal experiments suggests that metastable, reversible alkane/alkene equilibrium should

165 be attained under hydrothermal conditions with half-equilibration times of several hundred hours or less at

166 temperatures of 325 to 350 °C (Seewald, 1994, 2001). Failure to achieve thermodynamic equilibrium within

167 these timescales indicates that generation of thermogenic alkenes occurs concurrently with alkane/alkene

168 hydrogen exchange. Various pyrolysis experiments have reported alkene production (Huizinga et al., 1987; Leif

169 and Simoneit, 2000), lending further support to the hypothesis that continued production of alkenes competes with

170 their conversion into alkanes via hydrogenation at these temperatures and timescales and under redox conditions

171 characterizing hydrothermal maturation of organic-rich mudrocks.

172 Unlike the C_{2+} alkanes, methane cannot dehydrogenate to form an alkene. Hence, hydrogen exchange of methane

173 requires that the very stable C–H bond be broken. Under certain conditions, generally requiring the absence of

174 water or other catalyst poisons, methane exchanges hydrogen over certain catalytic materials such as γ-alumina at

175 room temperature over hours to days (Sattler, 2018, and refs. therein; or with organometallic catalysts under even

176 colder conditions, Golden et al., 2001). However, such catalysts in their active forms are not known to occur

177 naturally in aqueous environments. Experiments conducted by Reeves et al. (2012) with aqueous methane in the

178 presence of iron-bearing minerals in similar flexible-cell Au-TiO_2 reaction vessels revealed only minimal

179 potential exchange over several months, even at temperatures as high as 323 °C. Recently, Turner et al.

180 (unpublished / under review) conducted a set of experiments in flexible gold-cell hydrothermal reactors with CH_4

181 dissolved in supercritical water at 376 to 420 °C to specifically constrain the rate of CH_4–H_2O hydrogen isotope

182 exchange. Their results confirm that exchange occurs over timescales of hundreds of years at 300 °C and tens of

183 years at 350 °C (half-exchange time, $\tau_{1/2}$), much longer than the duration of our experiment.

8

3.3. Production of deuterated methane isotopologues

Mass spectra collected for standards are shown in **Fig. 3**. Relative fragment intensities were similar to those determined in early studies from the U.S. National Bureau of Standards (Dibeler and Mohler, 1950; Mohler et al., 1958). Mass spectra of samples are shown in **Fig. 4**. No methane peaks of usable size could be obtained for time point #1. All other time points yielded quantifiable extracted ion chromatogram peaks.

The mass spectra of commercial standards were used to fit the sample data using a constrained linear least-squares solver (LSQNONNEG) implemented in MATLAB.[1] Estimated fractional abundances of methane-d isotopologues at each time point are shown in **Fig. 5A**.[2] While it is not straightforward to quantify the uncertainty in these fractional abundances, comparison of the calculated results for samples #6(1) and 6(2) suggests the random error is unlikely to be so large as to affect our interpretation of the overall trends below. Some systematic error is likely present as we did not correct the mass spectra for the ^{13}C isotope or for isotopic impurities in the standards. Fractional abundances for each of the isotopologues were converted into absolute abundances (**Fig. 5B**) by multiplying by the methane concentration. The proportion of D in methane-bound hydrogen, calculated from the relative isotopologue abundances, is shown in **Fig. 6**.

Methane formed during the early stages of the experiment at 200 °C was primarily C^{1}H$_4$ with some CH$_3$D, whereas at higher temperatures, the isotopologues produced consisted almost exclusively of CD$_4$, CHD$_3$, and CH$_3$D (**Fig. 5A** and **Fig. 6**). These results suggest that at relatively lower temperatures of ~200 °C, the rate of methane generation approaches or exceeds the rate of D/H exchange between water and kerogen, whereas at higher temperatures, extensive D/H exchange between kerogen (or ~~oils~~ petroleum, if they are ~~also precursors~~ also a precursor of methane) and water occurs prior to methane generation. CD$_4$ became the dominant methane species at temperatures of 300 °C and above, suggesting that more than 50% of all labile, methane-generating sites on kerogen were fully

---

[1] This deconvolution scheme has been used to derive concentrations of methane-d isotopologues from mass spectral data for a separate experimental exchange study (A. Sattler, pers. comm.).

[2] Results of this experiment were first presented in the appendix of a Ph.D. thesis (Wang, 2017). That earlier analysis contained a mathematical error (neglected to divide by the relative peak areas of the pure isotopologue standards). As a result, Fig. B.3 of that thesis appears different than **Fig. 5** in this paper.

Author: Subject: Highlight Date: 4/21/2022 4:10:14 AM
Consider combining Fig. 3 and 4 into a single figure

Author: Subject: Inserted Text Date: 4/21/2022 4:14:21 AM
it

Author: Subject: Inserted Text Date: 4/21/2022 4:42:13 AM
petroleum

Author: Subject: Inserted Text Date: 4/21/2022 4:42:33 AM
also a precursor

205   deuterated by this time. As discussed above, uncatalyzed CH_4–D_2O isotopic exchange at this temperature occurs

206   over a much longer timescales than the short (~1 month) duration of our laboratory experiment . There is a

207   possibility of mineral catalysis on the surfaces of the source rock powder used in the experiment, which we cannot

208   rule out given the setup of our experiment. However, the minimal degree of isotopic exchange observed by

209   Reeves et al. (2012) at temperatures of 323 °C and timescales of ~1 year in the presence of redox-active minerals

210   (pyrite, pyrrhotite, and magnetite) suggests that direct exchange of CH_4 with D_2O in our experiment is probably

211   unimportant.

212   Production of C^1H_4 in the first stage of the experiment (200 °C) indicates that the earliest "capping" hydrogen

213   derives from kerogen or other H-containing species in the rock as opposed to from the H atoms of water. This

214   can only be the case if kerogen has not yet undergone D/H exchange.[3] While constraints on timescales of D/H

215   exchange at 200 °C are sparse, the available literature supports this assertion. Experiments conducted with model

216   hydrocarbons indicate that D/H exchange of carbon-bound H at 200 °C takes at least several decades, much

217   longer than the heating time in our experiment (Sessions et al., 2004; Schimmelmann et al., 2006; Sessions, 2016;

218   and refs. therein).

219   Production of C^1H_4 and CH_3D appeared to cease by midway through the 300 °C stage (time point #4, 284 hours),

220   or was overshadowed by the generation of much larger quantities of the higher isotopologues. Continued (though

221   relatively minor) production of methane that was not fully-deuterated (CHD_3 and CH_3D, **Fig. 5B**) suggests that

222   the kerogen (or ~~oil~~) from which methane was generated still did not fully exchange before methane formed.

223   If significant exchange were to occur, either between water and kerogen, or between water and methane generated

224   by thermal degradation of longer chain products, and this exchange occurs sequentially, the predominant

225   isotopologue would be expected to follow the progression $C^1H_4 \rightarrow CH_3D \rightarrow CH_2D_2 \rightarrow CHD_3 \rightarrow CD_4$. Instead,

226   CH_2D_2 represents a smaller fraction of the methane isotopologues than either CH_3D or CHD_3 at all times, and

---

[3] It is conceivable that the C^1H_4 observed at time point #2 may have been gas originally present but sorbed to a solid phase at the start of the experiment and later leached into the fluid, but we consider this unlikely because Soxhlet extraction should have removed nearly all of the CH_4 initially sorbed. Furthermore, the concentration of methane tripled between time points #1 (19 h) and #2 (164 h). Release of sorbed gases was probably nearly complete by 19 h.

Author: Subject: Highlight Date: 4/21/2022 4:29:31 AM
But the source rock matrix is likely important as a catalyst for the exchange of kerogen-bound H with D2O (prior to methane generation) - I think it's important to clarify this point.

Author: Subject: Inserted Text Date: 4/21/2022 4:42:55 AM
petroleum

227   calculated proportions of CH_2D_2 do not exceed 10% at any point in the experiment (**Fig. 5A**). A possible

228   explanation is that various CH_x moieties (e.g., aromatic C vs. methylene C vs. heteroatom-bound C) of the

229   kerogen or generated petroleum may have significantly different propensities to undergo exchange and

230   hydrogenation. Thermal degradation that occurs much slower or faster than exchange may yield either fully-

231   deuterated kerogen (e.g., –CD_3) or singly-deuterated methane, respectively, hence leading to an absence of

232   CH_2D_2. Alternatively (or possibly in addition), D/H exchange of partially-deuterated longer-chain hydrocarbon

233   molecules with water may be faster than degradation, such that the production of CH_2D_2 is "skipped". The

234   selective production of deuterated methane isotopologues is additional evidence that exchange between

235   water/methane or methane/methane at temperatures of 200 to 350 °C is slow on timescales relevant to laboratory

236   experiments.[4]

237   Comparison of our results with those of Wei et al. (2019), who examined CH_4 generation from petroleum source

238   rock heated under hydrothermal conditions, reveals similar thermal maturity trends for the extent of CH_4

239   deuteration (**Fig. 6A**). Both studies yielded methane with an increasing percentage of water-derived hydrogen as

240   thermal maturity increased. The deuteration vs. maturity trends are sub-parallel to each other. The observed

241   offset between the Wei et al. experimental results and ours is probably due to the different source rocks and

242   experimental conditions, including the use of D_2O instead of normal water as the aqueous medium in our

243   experiments. By the middle of the oil window (0.75–0.9% R_o), methane in both studies contained more than 50%

244   of its hydrogen content derived from water.

245   The percentage of methane deuteration as a function of cumulative CH_4 generated is shown in **Fig. 6B**.[5] Because

246   approximately 100 μmol of CH_4 was generated in total, the *x*-axis of this panel can be read as % of cumulative

247   methane generation. At 50% deuteration, only less than 10% of methane has been generated. Stated another way,

248   for 90% of the total methane generated in the experiment, more than half of its H content comes from water.

---

[4] This might be verified by heating normal water (^1H_2O) in the presence of an initial charge of CD_4 and monitoring for any increase in the δD value of water.

[5] Calculated as $[CH_4] \times V_{remaining} + \sum ([CH_4] \times V_{withdrawn})$.

294 *3.4.2. D/H exchange in precursor organic molecules*

295 In maturing and thermally-mature source rocks, kerogens can be expected to have exchanged part of their organic

296 hydrogen pool with ambient waters. In experiments on source rocks heated to 310–381 °C for up to 6 days with

297 deuterium-enriched and deuterium-depleted waters, Schimmelmann et al. (1999) found that 45 to 79% of carbon-

298 bound hydrogen was derived from water after pyrolysis to equivalent maturities as high as ~1.3% (as

299 EASY%Ro). Aliphatic Type I kerogen, containing large amounts of alkyl groups, were noted to be more

300 isotopically-conservative than kerogens with greater amounts of NSO-containing moieties such as Type IIS

301 kerogen.

302 Exchange of *n*-alkyl hydrogens is slow relative to hydrogen exchange at other positions such as at the α-carbons

303 of C=O groups (Sessions et al., 2004). However, exchange rates for aliphatic hydrogens are not zero. Exchange

304 may proceed via hydrogen transfer to a relatively stable tertiary carbocation-containing intermediate from

305 adjacent methyl or methylene groups (Alexander et al., 1984), or via the reversible dehydration of alkanes to form

306 alkenes under conditions of metastable equilibrium (Seewald, 1994; Reeves et al., 2012). In the absence of

307 significant direct CH_4–H_2O exchange, the formation of large amounts of CD_4 during our experiment suggests that

308 the hydrogen at methyl groups of kerogen (or in other alkyl precursors) exchanges with water under thermal

309 conditions compatible with the generation of petroleum (**Fig. 7B–C**). Water is abundant within most source

310 rocks, with even source rocks with very low water saturation containing up to several percent water by weight

311 (Kazak and Kazak, 2019). Hence, substantial incorporation of water-derived H into CH_4 is likely to occur in

312 actively-generating source rocks so long as water is in contact with sedimentary organic matter. Water dissolved

313 in bitumen generated from kerogen decomposition may participate in CH_4 generation (Lewan and Roy, 2011), as

314 well as water located in pore spaces that are at least partially-lined with organic matter (see §3.5). Equilibrium

315 D/H fractionation between organics and water is likely to be readily attained in at least several functional groups

316 during kerogen maturation. While different equilibrium fractionation factors characterize the various H positions

317 in different *n-* and branched alkanes, the average D/H fractionation for *n*-alkanes trends in the same direction as

318 methane (i.e., alkane δD lower than water) (Wang et al., 2009). The progressive incorporation of pre-equilibrated

14

319 alkyl H into thermogenic methane during natural gas generation may explain in part the approach towards

320 apparent equilibrium with formation water seen in CH_4 of increasing thermal maturity (Clayton, 2003; Wang et

321 al., 2018; Turner et al., 2021).

322 *3.4.3. D/H exchange between methane and water in conventional vs. unconventional reservoirs*

323 Timescales of direct hydrogen exchange between CH_4 and ambient H_2O based on experiments conducted in the

324 absence of catalyst range from hundreds of thousands of years at temperatures around 200 °C, up to hundreds of

325 millions of years at temperatures below 150 °C (Koepp, 1978; Reeves et al., 2012; Wang et al., 2018; Beaudry et

326 al., 2021; Turner et al., under review).

327 In a conventional petroleum system, hydrocarbons are generated within an organic-rich source rock, expelled

328 from the source rock into permeable carrier beds, and transported along carrier beds to a reservoir or seep.

329 Generation of oil typically occurs at 80–160 °C (the 'oil window'; **Fig. 8A**). Oil remains within the organic matrix

330 until the amount of retained oil exceeds the expulsion threshold (typically considered a function of organic

331 richness) prior to being expelled from the source rock (Sandvik et al., 1992). Oil-prone source rocks will tend to

332 expel most of their generated hydrocarbons relatively soon after generation, whereas in leaner source rocks with

333 less generative potential, generated oil mostly remains trapped in the source rock (Cooles et al., 1986). In the

334 latter case, larger hydrocarbon compounds (C_{15+}) will have ample time to both undergo exchange of its carbon-

335 bound H (Sessions et al., 2004) and degrade to smaller compounds such as CH_4 that can more easily escape the

336 source rock (Cooles et al., 1986). Expulsion of light hydrocarbons (C_{15} or below, including the $C_1–C_5$ gases) is

337 geologically rapid, particularly if the source rock comprises relatively thin (meter-scale) organic-rich beds

338 interbedded with permeable silts or sands (Mackenzie et al., 1983). Secondary migration (from source rock to

339 reservoir) is likely fast as well, even if such migration occurs over long lateral distances (~25 km) (<200,000

340 years for the L.A. Basin; Jung et al., 2015; see also Hindle, 1997; Eichhubl and Boles, 2000). Given that

341 reservoirs are most often cooler than the source rocks, the C–H bonds in CH_4 will have been 'frozen' at or near the

342 point of generation for methane generated at temperatures below ~170 °C. This is easily demonstrated using

343 forward models of isotopic exchange such as those shown by Wang (2017, Appendix A) for clumped

15

344 isotopologues of CH$_4$ in conventional gases under conservative assumptions about cooling during migration.

345 Methane generated in source rocks at temperatures above the oil window will be more likely to approach D/H

346 equilibrium with water, even if it migrates immediately after generation. The dataset presented by Clayton (2003)

347 showing a leveling-off of δD(CH$_4$) values at around −140 to −150‰ in higher maturity, conventional, oil-

348 associated gases while δ^{13}C(CH$_4$) continues to increase is very supportive of exchange having occurred at

349 temperatures of >170 °C within or proximal to the source rocks.

350 By contrast, extensive hydrogen exchange in CH$_4$ likely proceeds post-generation for unconventional petroleum

351 systems where the source rocks are also the reservoirs. In these self-sourced systems, CH$_4$ that remains entrapped

352 in pore spaces will probably have exchanged hydrogens with surrounding organics or with any available water as

353 long as the rock has been exposed to temperatures of at least ~130 °C at maximum burial. This is supported with

354 observations that at elevated maturities, CH$_4$ approaches isotopic equilibrium with co-existing formation waters in

355 unconventional reservoirs such as the Utica, Marcellus, and Eagle Ford, consistent with transfer of H from paleo-

356 groundwaters to methane (Wang et al., 2015; Xie et al., 2021).

357 **3.5. Generation potential of natural gas**

358 Volumetric calculations based on source rock extent, type, richness, and maturity are used to estimate the mass of

359 hydrocarbons generated by source rocks undergoing thermal maturation. These calculations are the basis of

360 estimates of potential resources when assessing frontier basins when only coarse constraints on source rock

361 presence and character are available (Schmoker, 1994). They are also formalized as programmatic subroutines

362 embedded in modern basin modeling packages (Tissot and Espitalié, 1975; Cooles et al., 1986; Pepper and Corvi,

363 1995; Tissot, 2003; Freund et al., 2007; Hantschel and Kauerauf, 2009; Stainforth, 2009; Fjellanger et al., 2010)

364 which take spatially-resolved hydrogen index (HI) values of source horizons as a key input constraint.

365 In a series of experiments, Wenger and Price (1991) heated shale source rocks and coals in the presence of water

366 for 30 days at temperatures of 150 to 500 °C. They observed that HI values often increased with experimental

367 temperature, instead of declining as would be expected for simple depletion of initial kerogen via cracking

16

Author: Subject: Inserted Text   Date: 4/22/2022 2:04:46 AM
thermal

Author: Subject: Inserted Text   Date: 4/22/2022 2:05:12 AM
thermal

Author: Subject: Inserted Text   Date: 4/22/2022 2:05:45 AM
thermal

368 reactions. Furthermore, more hydrocarbons were generated in some experiments than the theoretical maximum

369 yield expected if H in generated petroleum was only derived from organic matter (Price, 2001, their Figure 3).

370 This excess hydrocarbon yield was attributed to incorporation of H_2O-derived hydrogen during the hydrolytic

371 disproportionation of kerogen into $CO_2 + CH_4$ and other small paraffins, consistent with theoretical and

372 experimental constraints on petroleum degradation in aqueous environments (Helgeson et al., 1993, 2009;

373 Seewald, 1994, 2001, 2003).

374 Evidence from our results and the other studies discussed above suggest that hydrocarbon generation in source

375 rocks may not be limited by the hydrogen content of source kerogen. Hence, if H availability is not limiting, and

376 water participates in the formation of hydrocarbons, the upper bound on the amount of hydrocarbons that can be

377 generated is the availability of water to petroleum-generating reactions up to the point of TOC exhaustion. This

378 has been repeatedly suggested by several authors in years past (Lewan, 1992; Helgeson et al., 1993, 2009; Price,

379 1994, 2001; Seewald, 1994, 2003). If correct, kinetic models of petroleum formation employed in basin modeling

380 that limit hydrocarbon yields based on HI values (Tissot et al., 1987; Tissot, 2003; Hantschel and Kauerauf, 2009)

381 may significantly underpredict the true natural gas resource potential in many of the world's sedimentary basins

382 (**Fig. 8**).

383 Several important differences between experimental hydrothermal pyrolysis of source rock powder and

384 maturation of source rocks in nature bear discussing. Most obviously, laboratory experiments substitute higher

385 temperatures to permit hydrocarbons to be generated within much shorter timescales than in nature. Hence, for

386 extrapolation from laboratory to geologic conditions, it is implicitly assumed that the same chemical reactions

387 occur in the same proportions at high and low temperatures. Experiments indicate that this is not often the case,

388 particularly for individual compositional groups (Snowdon, 1979; Ungerer and Pelet, 1987; Dieckmann et al.,

389 2000; Schenk and Dieckmann, 2004). Results of experimental studies, including this one, must be interpreted

390 with this in mind.

Author: Subject: Cross-Out Date: 4/22/2022 2:12:52 AM

391   The availability of water to natural gas-generating reactions may also differ between experiment and nature. Our

392   experiment was set up with a comparatively high water:rock ratio (5:1) to allow ease of sampling, to maintain

393   single-phase conditions, and to prevent dilution of the deuterium content of the water by exchange with rock. The

394   water:carbon ratio was concomitantly high, approximately 200:1 given the TOC of 2.5% and ignoring mineral

395   carbon which is assumed to not participate in the generation of thermogenic methane. Grinding the Eagle Ford

396   rock sample to rock powder allowed water to readily access exposed sedimentary organic matter with ease. By

397   contrast, petrophysical studies of the structure of pore systems within clay-rich, organic-rich, overmature gas

398   shales suggest that much of the water is bound to the surfaces of clay minerals and contained predominantly in

399   interstices between clay mineral grains (see Figure 30 in Passey et al., 2010). This clay-adsorbed "irreducible

400   water" is considered immobile and cannot be produced during extraction of hydrocarbons, whereas free or

401   capillary-bound water is mobile and comes comingled with gas and oil during production. Using a rastering

402   scanning electron microscopy (SEM) technique, Passey et al. (2010) imaged overmature shale source rocks in 3D,

403   finding abundant small (<0.1 μm) bubble-shaped pore spaces within the organic matter and observing that this

404   intra-organic porosity tended to be interconnected yet isolated from the water-bearing intergranular matrices.

405   While the physical separation of gas-containing pockets from water-bearing interstitial spaces alone might suggest

406   that contact between water and organic material is limited, two processes must be considered. Firstly, much of

407   the oil and gas generated at or near grain boundaries probably underwent primary migration and was expelled out

408   of the source rock long before the present day (Mackenzie et al., 1983; Cooles et al., 1986; Sandvik et al., 1992).

409   Hence, the absence of gas in contact with water does not necessarily indicate that water was unavailable during oil

410   and gas generation. This is supported by more recent SEM work suggesting that a substantial amount of the water

411   fraction in shale source rocks may have direct contact with organic matter that commonly exists within interstices

412   of clay minerals (Gupta et al., 2018). The second consideration is that trapped water may have been initially

413   present and was quantitatively consumed during the generation of the gas now present in the organic porosity.

414   This is analogous to water trapped within mineral interstices in partially-serpentinized peridotitic rock at mid-

415   ocean ridges reacting with the olivine minerals that surround it, resulting in often dry (waterless), H_2- and CH_4-

416   rich gas secondary fluid inclusions (Klein et al., 2019; Grozeva et al., 2020). Each individual fluid inclusion (or

697   ~~Turner, A.C., Pester, N.J., Bill, M., Conrad, M.E., Knauss, K.G., Stolper, D.A., unpublished / under review~~

698   ~~Experimental determination of hydrogen isotope exchange rates between methane and water under~~

699   ~~hydrothermal conditions. Geochimica et Cosmochimica Acta.~~

700   ~~Turner, A.C., Pester, N.J., Bill, M., Conrad, M.E., Knauss, K.G., Stolper, D.A., under review. Experimental~~

701   ~~determination of hydrogen isotope exchange rates between methane and water under hydrothermal~~

702   ~~conditions. Geochimica et Cosmochimica Acta.~~

703   Ungerer, P., Pelet, R., 1987. Extrapolation of the kinetics of oil and gas formation from laboratory experiments to

704   sedimentary basins. Nature 327, 52–54.

705   Vinnichenko, G., Jarrett, A.J.M., van Maldegem, L.M., Brocks, J.J., 2021. Substantial maturity influence on

706   carbon and hydrogen isotopic composition of n-alkanes in sedimentary rocks. Organic Geochemistry 152,

707   104171.

708   Wang, D.T., 2017. The geochemistry of methane isotopologues (PhD Thesis). Massachusetts Institute of

709   Technology and Woods Hole Oceanographic Institution. doi:10.1575/1912/9052

710   Wang, D.T., Gruen, D.S., Lollar, B.S., Hinrichs, K.-U., Stewart, L.C., Holden, J.F., Hristov, A.N., Pohlman, J.W.,

711   Morrill, P.L., Könneke, M., Delwiche, K.B., Reeves, E.P., Sutcliffe, C.N., Ritter, D.J., Seewald, J.S.,

712   McIntosh, J.C., Hemond, H.F., Kubo, M.D., Cardace, D., Hoehler, T.M., Ono, S., 2015. Nonequilibrium

713   clumped isotope signals in microbial methane. Science 348, 428–431.

714   Wang, D.T., Reeves, E.P., McDermott, J.M., Seewald, J.S., Ono, S., 2018. Clumped isotopologue constraints on

715   the origin of methane at seafloor hot springs. Geochimica et Cosmochimica Acta 223, 141–158.

716   Wang, Y., Sessions, A.L., Nielsen, R.J., Goddard III, W.A., 2009. Equilibrium $^2H/^1H$ fractionations in organic

717   molecules. II: Linear alkanes, alkenes, ketones, carboxylic acids, esters, alcohols and ethers. Geochimica

718   et Cosmochimica Acta 73, 7076–7086.

719   Wei, L., Gao, Z., Mastalerz, M., Schimmelmann, A., Gao, L., Wang, X., Liu, X., Wang, Y., Qiu, Z., 2019.

720   Influence of water hydrogen on the hydrogen stable isotope ratio of methane at low versus high

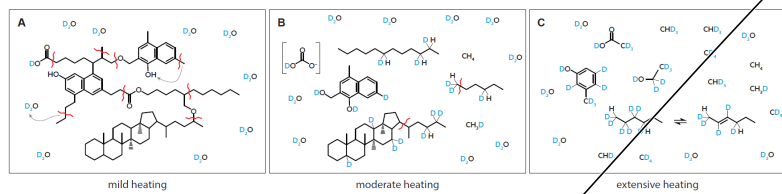721   temperatures of methanogenesis. Organic Geochemistry 128, 137–147.

773   mild heating   moderate heating   extensive heating

774   **Fig. 7.** Cartoon showing process of sequential deuteration of kerogen and oil along with generation of deuterated methane. Snapshots shown

775   represent stages of (A) mild heating (incipient catagenesis); (B) moderate heating (oil generation); and (C) extensive heating (gas window).

40